

## Article

# Research on the Inhibitory Effect of Hydrated Phase Change Materials on Spontaneous Combustion in Coal

Fanghua Wu, Shiliang Shi \*, Shuzhen Shao, Yi Lu, Wangxin Gu, Youliang Wang and Xindi Yuan

School of Resource, Environment and Safety Engineering, Hunan University of Science and Technology, Xiangtan 411201, China; 19010102001@mail.hnust.edu.cn (F.W.); kangwd12@hnust.edu.cn (S.S.); 1010088@hnust.edu.cn (Y.L.); zsj@hnust.edu.cn (W.G.); gaorg@hnust.edu.cn (Y.W.); zhangzuobin@hnust.edu.cn (X.Y.)

\* Correspondence: 1010111@hnust.edu.cn

**Abstract:** In order to study the effect of hydrated phase change materials on the suppression of spontaneous combustion in coal, a thermogravimetric experiment and a reaction activation energy analysis experiment were conducted to explore the changes in the combustion characteristic parameters, characteristic temperature, and activating energy of gas coal, long-flame coal, meagre coal, and lean coal before and after adding hydrated phase change materials. The research results indicated that hydrated phase change materials increased the characteristic temperature point of the coal samples and had effective inhibitory effects on different stages of the oxidation process. However, the effect was best at low temperatures, as hydrated phase change materials undergo phase change and absorb heat when heated at low temperatures, isolating coal from contact with oxygen. The activating energy increased by 1.138–23.048  $\text{KJ}\cdot\text{mol}^{-1}$  and the mass loss was reduced by 1.6%–9.3% after inhibition of the coal samples, indicating that the oxidation rate of the various coal samples was slowed down and, thus, spontaneous combustion can be suppressed through the use of hydrated phase change materials. At the same time, this material reduced the combustibility indices of meagre coal and lean coal, as well as the comprehensive combustion indices of long-flame coal and gas coal.

**Keywords:** hydrated phase change materials; coal spontaneous combustion; thermogravimetric; activating energy; inhibitory effect; combustibility index; comprehensive combustion index



**Citation:** Wu, F.; Shi, S.; Shao, S.; Lu, Y.; Gu, W.; Wang, Y.; Yuan, X. Research on the Inhibitory Effect of Hydrated Phase Change Materials on Spontaneous Combustion in Coal. *Fire* **2024**, *7*, 95. <https://doi.org/10.3390/fire7030095>

Academic Editor: Ali Cemal Benim

Received: 15 January 2024

Revised: 12 February 2024

Accepted: 15 February 2024

Published: 17 March 2024



**Copyright:** © 2024 by the authors. Licensee MDPI, Basel, Switzerland. This article is an open access article distributed under the terms and conditions of the Creative Commons Attribution (CC BY) license (<https://creativecommons.org/licenses/by/4.0/>).

## 1. Introduction

Due to the characteristics of energy storage in China, coal has always held a relatively important position in China's energy consumption [1–3]; however, coal has a natural tendency to spontaneously combust under certain conditions. There is more residual coal in a goaf due to increased mining intensity, coupled with severe air leakage, raising the possibility that the residual coal self-ignites. The spontaneous combustion of coal can lead to huge economic losses [4]. Therefore, the mechanism underlying the spontaneous combustion of coal must be investigated in order to guarantee the safety of coal mine production [5,6]. According to the most widely accepted coal oxidation hypothesis by scholars, both domestically and internationally [7], the process through which coal's reaction groups react with oxygen to produce heat is known as spontaneous combustion. This process increases the temperature of coal, accelerates the oxidation reaction, and generates more heat overall. When the heat accumulates and reaches the combustion temperature, the coal will undergo combustion. Therefore, controlling the release of heat during coal oxidation in the low-temperature stage is particularly important. According to previous research, the existing measures to prevent the spontaneous combustion of coal have been designed from two aspects—endothermic cooling and oxygen isolation—including the use of grouting [8], injecting gel [9], inert gas [10,11], and spraying inhibitor [12–14]. Among these measures, many scholars are interested in inhibitors as they effectively prevent coal from spontaneously combusting. To date, various inhibitors—including physical and chemical

inhibitors—have been developed and applied on site both domestically and internationally, and their performance has been studied.

Huang [15,16] used a controlled temperature experimental system to examine the inhibiting effect of an inhibitor on the oxidation and spontaneous combustion of coal samples. They also examined the inhibition rates of coal samples at various temperature points. Dong [17] examined the inhibiting effect of an Enteromorpha-based composite inhibitor on the spontaneous combustion of coal samples using in situ Fourier infrared spectroscopy and thermal analysis kinetics. It was discovered that coal samples treated with inhibitors had an increase in average activating energy, raising their resistance to spontaneous combustion. The treated coal sample exhibited a higher content of -OH, compared with the raw coal sample. Wang [18] used infrared spectroscopy and temperature programming to examine the inhibitory effectiveness of polyethylene glycol–citric acid as an inhibitor. The findings demonstrated that polyethylene glycol–citric acid prevented the synthesis of CO and C<sub>2</sub>H<sub>4</sub>, the consumption of oxygen, and the oxidation of -CH<sub>3</sub> and -CH<sub>2</sub>. Gao [19] examined the impact of antioxidant-reduced glutathione on the tendency of coal to spontaneously combust using cross-point temperature and thermogravimetric differential scanning calorimetry, through which it was discovered that antioxidant-reduced glutathione had the ability to prevent coal from spontaneously combusting. Xue [20] utilized electron spin resonance and scanning electron microscopy to clarify the inhibition mechanism of an antioxidant-type composite inhibitor on coal oxidation. Pan [21] used a C600 microcalorimeter to examine the mechanism and inhibitory impact of an inhibitor on the oxidation heat release process in the spontaneous combustion of coal.

The spontaneous combustion of coal typically takes 1–3 months to develop. After this time, physical inhibitors may be unable to perform the functions of oxygen insulation and cooling due to water loss, while chemical inhibitors will lose functionality due to oxidization through exposure to the air [22,23]. The use of a phase change material inhibitor can ensure that its inhibition effect is not weakened over the long latent period, and, when the critical temperature is reached in the coal, phase change occurs to absorb coal heat, quickly and effectively closing the coal pores and isolating oxygen, thus moisturizing, cooling, and inhibiting the coal from entering the accelerated oxidation stage [24–26]. Therefore, in order to examine the inhibition effect of hydrated phase change materials on different coal types, this study uses hydrated phase change materials to inhibit four different coal types (i.e., gas coal, meagre coal, lean coal, and long-flame coal). The six characteristic temperatures of the samples are compared based on the results of thermogravimetric studies. Changes in the characteristic temperatures, activation energy, and combustion characteristic parameters of the coal samples before and after inhibition are analyzed, and the fire-extinguishing performance and advantages of the hydrated phase change materials are investigated.

## 2. Experimental Principle

According to existing research [27], when the temperature of coal reaches around 65 °C, the hydrated phase change material begins to undergo a phase transition, transforming from a solid to a fluid. The material gradually penetrates into the coal pores and cracks, but, at this point, it does not completely transform into a liquid. According to SEM results, the material has a large surface area, which can effectively seal cracks, prevent oxygen from entering, reduce the contact between coal and oxygen, and suppress the oxidation reaction that occurs during the spontaneous combustion of coal. When the temperature rises to 85 °C, the material undergoes a complete phase transition and can completely infiltrate the coal's body, envelop the coal seam, and achieve the effects of oxygen blocking and cooling.

By comparing the characteristic temperature changes associated with different coal grades during the entire combustion process before and after inhibition, the inhibitory effect of hydrated phase change materials on the spontaneous combustion of coal of different coal grades can be studied in order to better guide the application of hydrated phase change materials. The characteristic temperature is one of the most significant indicators of the intensity of the coal oxygen adsorption response, which quantifies the probability of coal

spontaneous combustion. The oxidation process may be broken down into four steps, based on the characteristic temperature of coal as follows: the stage of water loss and weight loss, the stage of oxygen absorption and weight growth, the pyrolysis stage, and the combustion stage. There are regular changes in mass loss during the coal combustion process, from initial decomposition to complete combustion to constant mass. The TG-DTG curves of experimental samples can be obtained through thermogravimetric experiments. The coal sample's weight change throughout the oxidation process is represented by the TG curve, and the DTG curve serves as a representation of the TG curve's rate of change (or its first-order derivative). It is mainly used to reflect the coal sample's weight change rate during the experimental process. By comparing the two curves, the variation rules of coal samples during the heating process can be accurately analyzed in order to determine the characteristic temperature points and different thermal oxidation phases of each coal sample as it is being heated. On this basis, the characteristic temperature changes in each combustion stage before and after coal sample inhibition can be compared, allowing for the inhibitory performance of hydrated phase change materials on coal spontaneous combustion to be ultimately determined.

### 3. Experimental Preparation and Scheme

#### 3.1. Treatment of Coal Samples

Four different grades of coal samples were selected and divided into meagre coal, lean coal, gas coal, and long-flame coal according to the volatile content (from low to high). Meagre coal was collected from Huagushan coal mine in Jiangxi Province, lean coal was collected from Shangzhuang coal mine in Jiangxi Province, gas coal was collected from Hongqi Coal mine in Shandong Province, and long-flame coal was collected from Donghuai coal mine in Guangxi Province. Table 1 shows the industrial analysis findings for the four coal samples. Among them,  $M_{ad}$  represents the moisture content,  $A_{ad}$  represents the ash content,  $V_{ad}$  represents volatile matter, and  $FC_{ad}$  represents fixed carbon.

**Table 1.** Results of industrial analysis.

Coal Sample	$M_{ad}/\%$	$A_{ad}/\%$	$V_{ad}/\%$	$FC_{ad}/\%$
Meagre coal	1.33	4.79	12.36	81.52
Lean coal	1.23	19.16	18.32	61.29
Gas coal	1.89	8.64	39.57	49.9
Long-flame coal	4.25	38.94	42.32	14.49

The preparation method for the experimental coal samples was to peel and core large coal samples collected on site. Nitrogen separation technology was used, and the samples were crushed. Then, using a 60–80 mesh, the coal ash was screened and stored as experimental coal samples in a drying oven to prevent physical and chemical adsorption in the air, leading to oxidation reactions.

The four experimental coal samples, which had varying degrees of metamorphism, were treated with a hydrated phase change material containing 57.6 wt% aluminum ammonium sulfate dodecahydrate [ $AlNH_4(SO_4)_2 \cdot 12H_2O$ , molecular weight: 453.15] and 42.4 wt% magnesium sulfate heptahydrate ( $MgSO_4 \cdot 7H_2O$ , molecular weight: 246.47). The weight ratio of coal samples to the resistance material was 4:1. After preparation, samples were left to stand for 12 h and then dried for 72 h in a vacuum drying oven at normal temperature. Finally, they were put into coal sample bags, sealed, and stored.

#### 3.2. Experimental Scheme

The thermogravimetric analysis method was adopted in this performance experimental test, for which a Shanghai Innuo TGA-1150 thermogravimetric analyzer was used, as shown in Figure 1.



Figure 1. TGA-1150 thermogravimetric analyzer.

The performance test experiment involved heating 8–10 mg of coal, with a temperature range of 40–1000 °C and rate of 10 °C/min. During the experiment, a gas composed of 78% N<sub>2</sub> and 22% O<sub>2</sub> was continuously injected at a rate of 0.1 L/min. The experimental data were obtained by setting the experimental parameters. Four coal samples with varying metamorphisms were evaluated for performance before and after inhibition, and the impact of the inhibitor on these coal samples was investigated [28].

#### 4. Experimental Result

##### 4.1. Characteristic Temperature Analysis

Each coal sample’s weight loss reflects how difficult it was to burn, as the weight loss is directly proportional to the completeness of combustion: the larger the weight loss, the easier it is for the coal sample to be burned completely. Similarly, it can be seen that the weight gain, which is related to oxygen uptake, is also proportional to the adsorption capacity of the coal samples. Figures 2 and 3 display the TG and DTG curves obtained in the experiment.

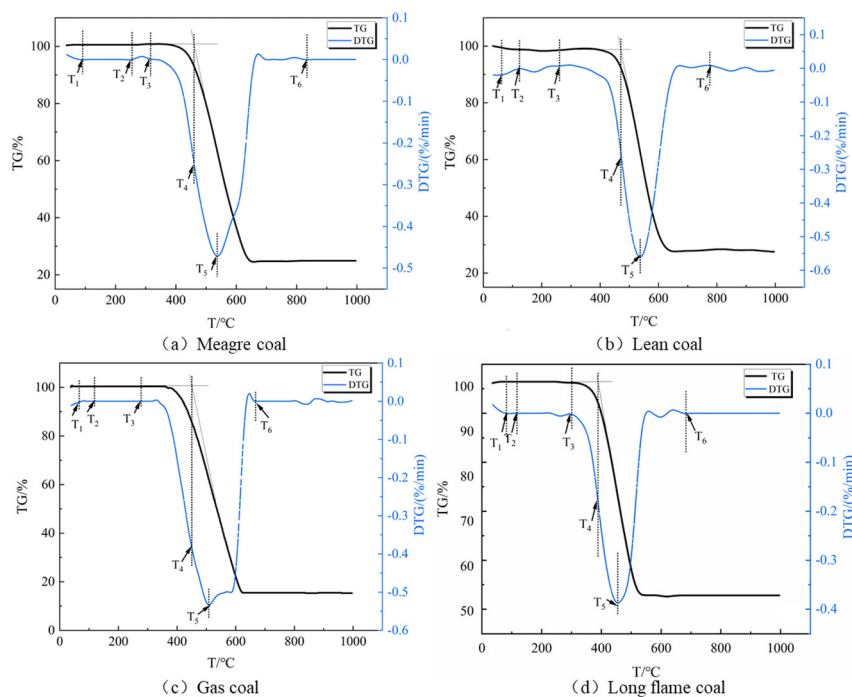


Figure 2. TG–DTG curves of various coal samples.

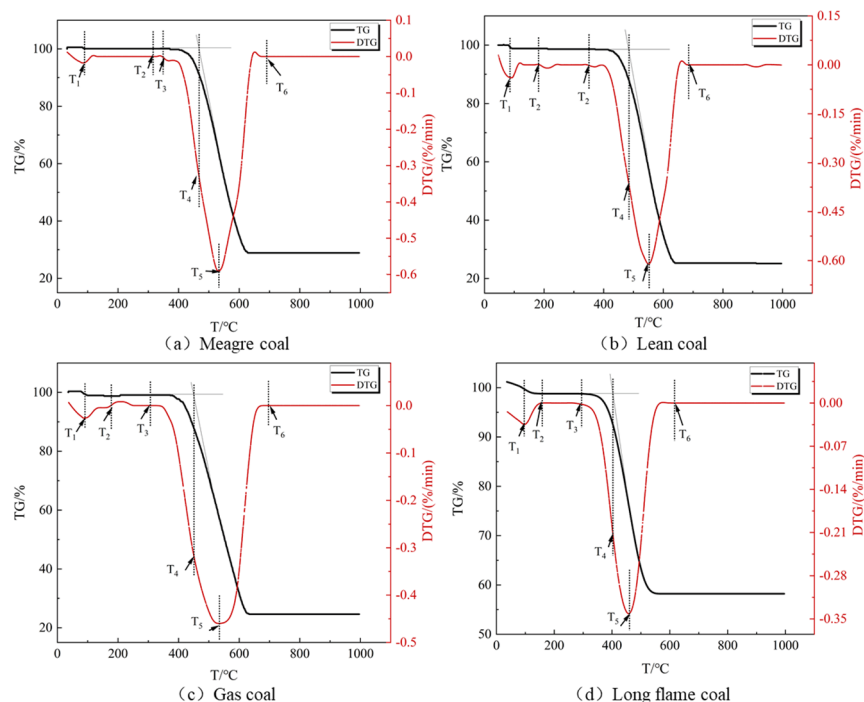


Figure 3. TG–DTG curves of various coal samples with inhibition.

Figures 2 and 3 show the variation curves for the various experimental coal samples throughout the oxidation heating process. Table 2 provides the characteristic temperature points and mass loss of each coal sample. The range of temperatures corresponds to each of the four oxidation processes as follows: the weight loss stage is  $T_1$ – $T_2$ , the weight gain stage is  $T_2$ – $T_3$ , the pyrolysis stage is  $T_3$ – $T_4$ , and the combustion stage is  $T_4$ – $T_6$ .

Table 2. Characteristic temperature point and mass loss of each coal sample.

Coal Sample	Characteristic Temperature						Mass Loss/%	
	$T_1/^\circ\text{C}$	$T_2/^\circ\text{C}$	$T_3/^\circ\text{C}$	$T_4/^\circ\text{C}$	$T_5/^\circ\text{C}$	$T_6/^\circ\text{C}$		
Raw coal sample	meagre coal	87.6	267.2	314.3	461.7	537.2	834.8	75.1
	lean coal	64.3	122.5	245.1	471.2	538.4	785.2	74.4
	gas coal	66.9	122.8	293.2	499.5	509.1	664.1	84.7
	long-flame coal	82.1	108.8	294.4	389.1	455.2	683.1	46.5
Inhibitory coal sample	meagre coal	90.2	316.9	341.3	467.5	536.6	691.8	71.1
	lean coal	84.6	180.9	352.8	485.2	548.9	687.8	72.8
	gas coal	90.3	180.3	305.3	452.5	535.7	678.7	75.4
	long-flame coal	96.2	160.8	298.2	403.6	463.5	612.9	41.7

Low-temperature oxidation of the coal sample took place under the thermogravimetric analyzer’s temperature program. While the water in the coal samples gradually evaporated, they adsorbed  $\text{O}_2$  and released  $\text{CO}$ ,  $\text{CO}_2$ , and other gases. In the beginning, the water evaporation rate was far greater than the  $\text{O}_2$  adsorption rate. Therefore, the weight loss rate in the coal sample continued to increase. When the critical temperature  $T_1$  was reached, the rate of weight loss in the coal sample peaked. As such,  $T_1$  corresponds to the DTG curve’s initial peak position, which was also the first temperature point at which the velocity of the coal–oxygen composite reaction increased [29]. The oxygen adsorptive capacity of the coal samples increased with temperature, while the thermal weight loss rate of the samples slowly decreased. When the water evaporation rate and the oxygen adsorption rate of the coal sample reached a dynamic equilibrium, the rate of thermal weight loss was 0. At this time, the water had essentially evaporated from the coal samples, and the dry cracking temperature  $T_2$  was reached [30]. At this time, some active groups started to react with  $\text{O}_2$

to generate oxygen-containing intermediates, which were stored in the coal sample, and the quality started to increase. When the temperature reached the thermal decomposition temperature  $T_3$ , the coal's weight gain rate due to oxygen absorption and its own reaction consumption rate reached dynamic equilibrium [31]. The thermal weight loss rate of the coal samples again became 0 and their mass growth rate was maximized, indicating the end of the weight gain stage. After reaching the pyrolysis temperature  $T_3$ , the coal sample was oxidized and decomposed, resulting in a significant reduction in quality. The internal energy of coal molecules increased as the temperature continued to increase, leading to the thermal decomposition of the circular structure inside the coal molecules. The quality of the coal samples continued to decrease and, after reaching the ignition temperature  $T_4$ , the coal sample started to burn [32]. After exceeding  $T_4$ , the coal sample presented a violent oxidation reaction, resulting in a significant quantity of gas being released and the primary coal molecular backbone structure being disrupted, which quickly reduced the coal sample's quality. After reaching the temperature  $T_5$ , the coal sample's thermal weight loss rate reached its maximum value. The maximum pyrolysis rate at temperature  $T_5$  on the DTG curve corresponded to the lowest point. At this time, the heated oxidation chemical decomposition reaction was the most intense, generating CO, CO<sub>2</sub>, H<sub>2</sub>O, and other trace gases. The active ingredient in the coal was basically consumed, and the combustion rate gradually decreased after this point. Until reaching the burnout temperature  $T_6$ , the quality of the coal samples tended to stabilize and no longer changed [33]. The TG-DTG curve inclined to a stable value at  $T_6$ , indicating that coal's oxidation and decomposition process had basically concluded.

Figure 4 shows the characteristic temperature changes in various coal samples before and after inhibition during the thermogravimetric experiment. After the coal samples were treated with hydrated phase change materials, their critical temperatures ( $T_1$ ) increased. Lower coal spontaneous combustion grade and lower coal body spontaneous combustion capacity were associated with higher critical temperatures. At low temperatures, hydrated phase change materials exhibited the most effective inhibitory effect on the spontaneous combustion of coal at temperatures ranging from 60 °C to 90 °C. This is because, at temperatures ranging from 60 °C to 90 °C, the hydrated phase change materials underwent a phase change when heated to the critical temperature point, thus maximizing heat absorption and reducing the rate at which coal's temperature increased, while also isolating oxygen from the coal, resulting in the prevention of spontaneous combustion. The inhibited lean and meagre coal samples had higher thermal decomposition temperatures  $T_3$  and dry cracking temperatures  $T_2$  than the raw coal. In the inhibited gas coal samples, the temperature  $T_5$  of the maximum thermal weight loss rate, the burnout temperature  $T_6$ , and  $T_2$  were all higher than those observed for the raw coal. The values of  $T_2$ , the ignition temperature  $T_4$ , and  $T_5$  for the inhibited long-flame coal sample were higher than those of the raw coal, indicating that the hydrated phase change material mainly acted on the stages of water loss, weight loss, oxygen absorption, and weight gain in meagre and lean coal. It also acted on the stages of water loss, weight loss, and combustion of gas coal and the stage of water loss, weight loss, and pyrolysis in long-flame coal.

The characteristic temperature points after inhibition were relatively lagging when the coal samples before and after inhibition were examined. Among them, the deviation in the critical temperature was the largest, indicating that hydrated phase change materials obtained an optimal result in the low-temperature phase of the self-heating oxidation process. The mass loss of the inhibited coal samples was 1.6–9.3% less than that in raw coal, and the rate of oxidation was slowed down. When the temperature of the coal body reaches the critical temperature of coal spontaneous combustion, the phase transition from a solid to a viscous fluid occurs, which can quickly and effectively seal the cracks in the coal, release water molecules to reduce the temperature of the coal body, isolate the contact between oxygen and coal, and delay the loss of water in the coal at low temperatures, thus greatly delaying the oxidation process of coal.

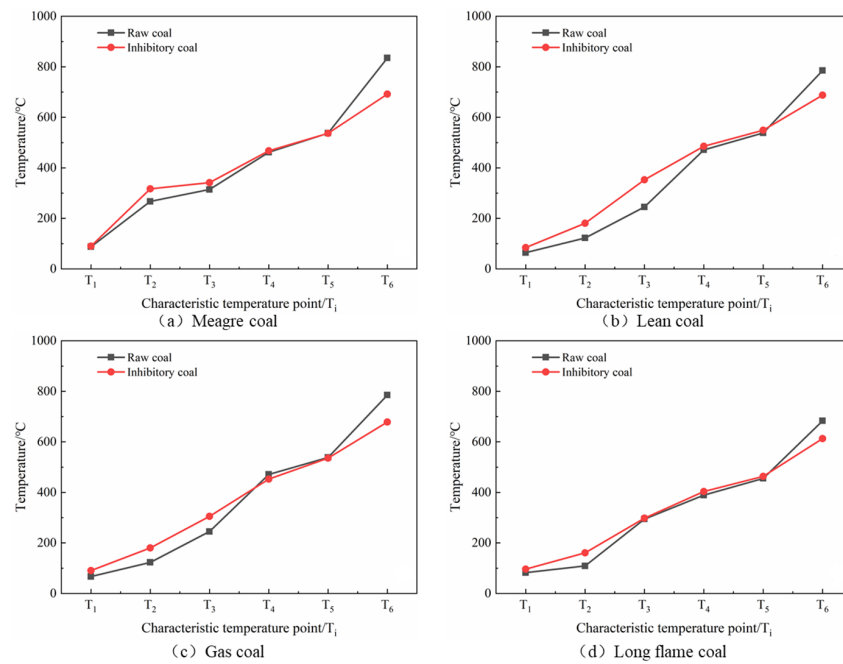


Figure 4. Characteristic temperatures of different coal samples before and after inhibition.

Therefore, in practical applications, in order to maximize the effectiveness of hydrated phase change materials, hydrated phase change materials can be sprayed onto the goaf from the upper and lower corners of the working face and the gaps between the working face supports during the low-temperature oxidation stage of residual coal in the goaf. The powder floats downward and upward in the cracks of the goaf along with the airflow of the goaf leakage zone, thus covering the entire goaf.

Figure 5 shows the weight loss rate and its reduction ratio observed in the thermogravimetric experiment before and after the inhibition of various coal samples. The calculation formula for the weight loss rate decrease ratio is shown in Equation (1):

$$\eta = \frac{S_a - S_b}{S_a} \tag{1}$$

where  $\eta$  is the weight loss reduction ratio, %;  $S_a$  is the weight loss rate before inhibition, %; and  $S_b$  is the weight loss rate after inhibition, %.

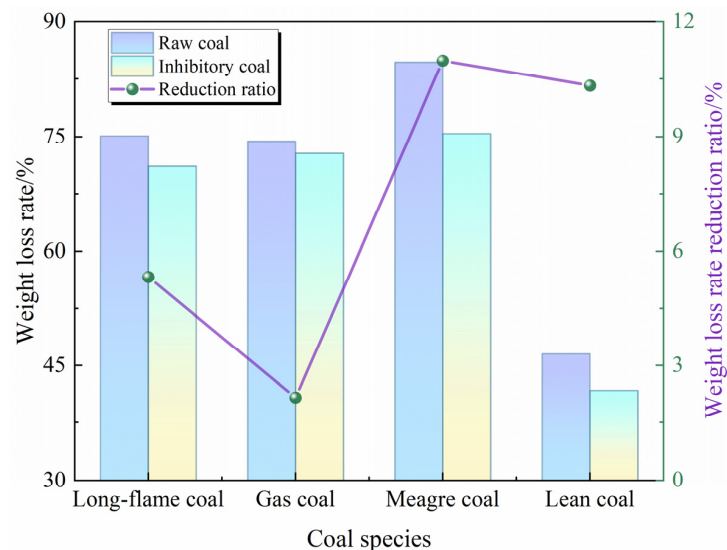


Figure 5. The weight loss rate and its reduction ratio before and after inhibition.

According to the characteristic temperature and weight loss rate before and after inhibition of coal samples, the hydrated phase change materials considerably reduced the weight loss rate in gas coal and long-flame coal, making them more appropriate for these types of coal.

#### 4.2. Combustion Characteristic Parameter Analysis

The parameters that describe the properties of coal combustion during combustion are called combustion characteristic parameters, which include combustion intensity, combustion difficulty, combustion rate, ignition performance, and burnout performance. They are typically used to reflect the coal's combustion state. The combustion characteristic parameters mainly include the flammability index and the comprehensive combustion characteristic index. At present, they are also used in research on mixed substances, flame-retardant materials, and non-coal materials during combustion.

- (1) The combustion intensity and difficulty of flammable materials are frequently assessed using the flammability index, which reflects their combustion rate, combustion performance, and so on. The flammability index is a key indicator that determines the performance of a combustible material in terms of ignition and combustion, where better ignition stability and combustion performance of flammable materials are indicated by higher flammability index values. The flammability index values obtained from performance testing experiment in this article were calculated from the maximum combustion rate and ignition temperature. As shown in Equation (2), the flammability index is directly inversely proportional to the square of the sample ignition point temperature and proportional to the sample's maximum combustion rate:

$$C = \frac{(dw/dt)_{\max}}{T_i^2} \quad (2)$$

where  $C$  is the flammability index,  $\% \cdot \text{min}^{-1} \cdot \text{K}^{-2}$ ;  $(dw/dt)_{\max}$  is the maximum mass loss rate,  $\%/ \text{min}$ ; and  $T_i$  is the ignition temperature,  $\text{K}$ .

- (2) When assessing the ability of combustible materials to ignite, the comprehensive combustion characteristic index is frequently employed, which reflects the quality of their combustion performance [34]. According to Equation (3), the sample's comprehensive combustion performance improves with a larger comprehensive combustion characteristic index value.

$$S = \frac{(dw/dt)_{\max} (dw/dt)_{\text{mean}}}{T_i^2 \cdot T_h} \quad (3)$$

where  $S$  is the comprehensive combustion characteristic index,  $\% \cdot \text{min}^{-1} \cdot \text{K}^{-3}$ ;  $(dw/dt)_{\text{mean}}$  is the average combustion rate,  $\%/ \text{min}$ ; and  $T_h$  is the burnout temperature,  $\text{K}$ .

The combustion characteristic parameters obtained through calculation are shown in Table 3. The flammability indices of the meagre and lean coal samples with hydrated phase change materials were added significantly decreased compared with the respective raw coal samples, while the comprehensive combustion characteristic index values were increased when compared with the raw coal samples. Compared with the raw coal samples, the inhibitory gas and long-flame coal samples displayed lower comprehensive combustion characteristic indices and higher flammability indices. The comprehensive combustion characteristic indices of gas and long-flame coal, as well as the flammability indices of meagre coal and lean coal, can all be lowered by adding hydrated phase change materials.

**Table 3.** Combustion characteristic parameters.

Coal Sample		$T_i/^\circ\text{C}$	$T_h/^\circ\text{C}$	$(dw/dt)_{\max}^l$ (%/min)	$(dw/dt)_{\text{mean}}^l$ (%/min)	C (%/min <sup>-1</sup> ·K <sup>-2</sup> )	S (%/min <sup>-1</sup> ·K <sup>-2</sup> )
Raw coal sample	meagre coal	461.7	834.8	−0.47	−0.081	$-8.704 \times 10^{-7}$	$6.36 \times 10^{-11}$
	lean coal	471.2	785.2	−0.56	−0.075	$-1.01 \times 10^{-6}$	$7.16 \times 10^{-11}$
	gas coal	499.5	664.1	−0.53	−0.102	$-8.88 \times 10^{-7}$	$9.66 \times 10^{-11}$
	Long-flame coal	389.1	683.1	−0.39	−0.049	$-8.89 \times 10^{-7}$	$4.56 \times 10^{-11}$
Inhibitory coal sample	meagre coal	467.5	691.8	−0.59	−0.085	$-1.08 \times 10^{-6}$	$9.65 \times 10^{-11}$
	lean coal	485.2	687.8	−0.61	−0.090	$-1.06 \times 10^{-6}$	$9.93 \times 10^{-11}$
	gas coal	452.5	678.7	−0.46	−0.089	$-8.74 \times 10^{-7}$	$8.17 \times 10^{-11}$
	Long-flame coal	403.6	612.9	−0.34	−0.045	$-7.42 \times 10^{-7}$	$3.77 \times 10^{-11}$

### 4.3. Reaction Activation Energy Analysis

In an atmospheric environment, coal will undergo oxidation and a spontaneous combustion reaction with air, which is usually called a gas–solid reaction. There are various phases in the coal spontaneous combustion process, and many small elements are involved in the reaction at each level. During the reaction process, a certain activation energy is required to overcome the corresponding energy barriers and transform them into activated molecules. According to calculation and analysis, the activation energy and the spontaneous combustion tendency of coal are related under certain conditions, and there is an inverse ratio between the two.

Based on the above research, using the thermogravimetric analysis method, we can study and analyze a coal body’s chemical process under changes in the temperature conditions or isothermal oxidation kinetics of solid materials. To determine the reaction’s activation energy, the Coats–Redfern integration method was used to process the thermogravimetric curve [35], and its oxidation reaction kinetics equation is expressed as follows:

$$\frac{d\alpha}{dT} = \left(\frac{1}{\beta}\right)k(T)f(\alpha) \tag{4}$$

where  $\beta$  is the heating rate;  $T$  is the thermodynamic temperature, K;  $f(\alpha)$  is the mechanism function describing the spontaneous combustion reaction of coal;  $k(T)$  is the reaction rate constant; and  $\alpha$  is the conversion rate of coal at time  $t$ , as shown in Equation (5):

$$\alpha = \frac{w_0 - w_t}{w_0 - w_\infty} \tag{5}$$

where  $w_0$  is the coal’s initial weight, mg;  $w_t$  is its weight at time  $t$ , mg; and  $w_\infty$  is its final weight, mg.

Arrhenius proposed that the rate constant and temperature have the following relationship:

$$k(T) = A \exp\left(-\frac{E}{RT}\right) \tag{6}$$

where  $E$  is the activation energy,  $\text{kJ}\cdot\text{mol}^{-1}$ ;  $A$  is the pre-exponential factor; and  $R$  is the gas molar constant,  $8.314 \text{ J}/(\text{mol}\cdot\text{K})$ .

Equation (7) is obtained by combining Equations (4) and (6).

$$\frac{d\alpha}{dT} = \frac{A}{\beta} \exp\left(-\frac{E}{RT}\right)f(\alpha) \tag{7}$$

Due to the low temperature at the beginning of the reaction, the reaction rate can be ignored. By integrating Equation (7), Equation (8) can be obtained:

$$\int_0^\alpha \frac{d\alpha}{f(\alpha)} = \frac{A}{\beta} \int_0^T \exp\left(-\frac{E}{RT}\right)dT \tag{8}$$

Equation (9) can be obtained by combining Equation (8) and the Coats–Redfern equation:

$$\ln \left[ \frac{G(\alpha)}{T^2} \right] = \ln \left[ \frac{AR}{\beta E} \left( 1 - \frac{2RT}{E} \right) \right] - \frac{E}{RT} \tag{9}$$

where  $G(\alpha)$  is the integral function of the reaction mechanism of the coal oxidation process, that is, the original function of  $\frac{1}{f(\alpha)}$ .

For the majority of  $E$  and the general response temperature range of coal samples,  $\frac{2RT}{E}$  is much smaller than 1; that is,  $1 - \frac{2RT}{E} \approx 1$ . Therefore, Equation (9) can be changed to Equation (10):

$$\ln \left[ \frac{G(\alpha)}{T^2} \right] = \ln \left( \frac{AR}{\beta E} \right) - \frac{E}{RT} \tag{10}$$

The general coal oxidation reaction is generally a first-order reaction, and the integral function of the reaction mechanism is usually  $\ln \left[ \frac{\ln(1-\alpha)}{T^2} \right]$ . Therefore, the coal oxidation reaction function obtained in this experiment is shown in Equation (11):

$$\ln \left[ \frac{\ln(1-\alpha)}{T^2} \right] = \ln \left( \frac{AR}{\beta E} \right) - \frac{E}{RT} \tag{11}$$

When  $\ln \left[ \frac{\ln(1-\alpha)}{T^2} \right]$  and  $\frac{1}{T}$  are plotted as a function graph, the slope on the graph is  $-\frac{E}{R}$ . The activating energy can be obtained through calculation. The intercept on the graph is  $\ln \left( \frac{AR}{\beta E} \right)$ , which can be calculated according to the pre-exponential factor. Figures 6 and 7 show the correlation analysis results for the oxidation reactions before and after inhibition in coal samples with four varying intensities of metamorphism.

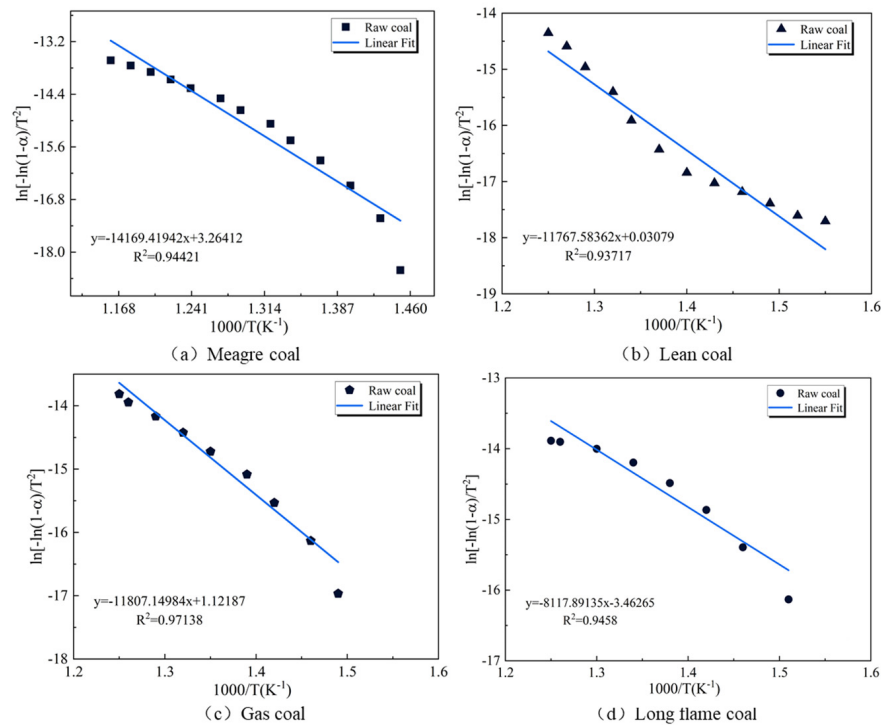


Figure 6. Correlation analysis of oxidation reactions of different raw coal samples.

A good association between the oxidation reactions of the four coal samples prior to and following inhibition was observed, with correlation coefficients greater than 0.9, indicating that the coal oxidation reaction was well-fitted with this function. As shown in Table 4, the pre-exponential factor and activating energy can be obtained through the fitting of equations.

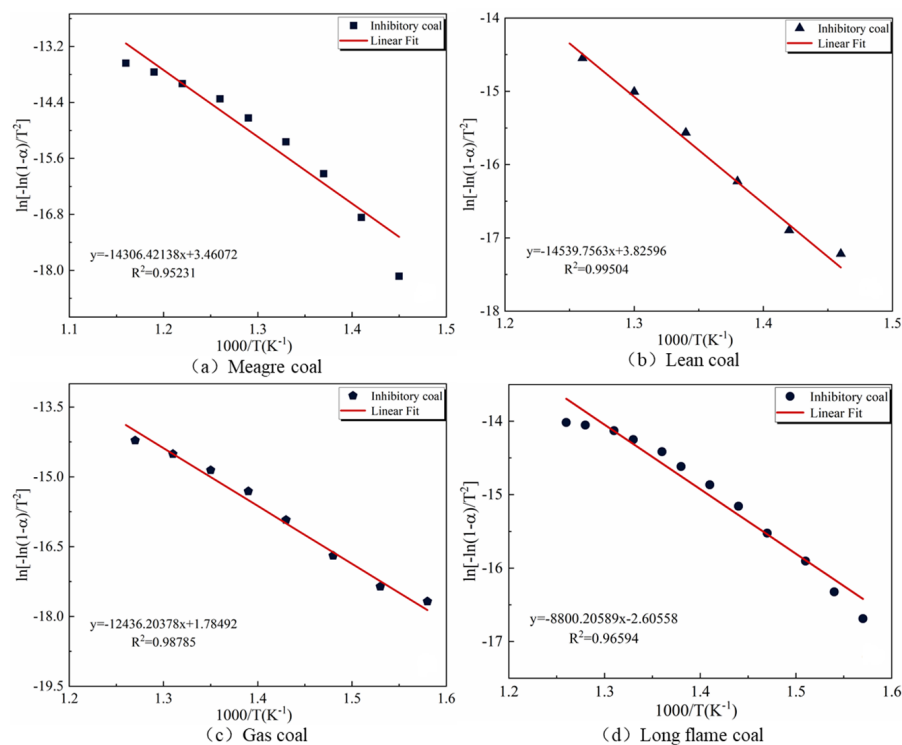


Figure 7. Correlation analysis of oxidation reactions of various inhibited coal samples.

Table 4. Kinetic parameters of oxidation reaction before and after coal sample inhibition.

Coal Sample		Related Coefficient	Fitted Equation	Activating Energy (KJ·mol <sup>-1</sup> )	Pre-Exponential Factor (10 <sup>5</sup> )
Raw coal sample	meagre coal	0.94421	$y = -14,169.41942x + 3.26412$	117.805	0.3706
	lean coal	0.93717	$y = -11,767.58362x + 0.03079$	97.836	0.0121
	gas coal	0.97138	$y = -11,807.14984x + 1.12187$	98.165	0.0363
	long-flame coal	0.94580	$y = -8117.89135x - 3.46265$	67.492	0.0003
Inhibitory coal sample	meagre coal	0.95231	$y = -14,306.42138x + 3.46072$	118.943	0.4555
	lean coal	0.99504	$y = -14,539.7563x + 3.82596$	120.884	0.6670
	gas coal	0.98785	$y = -12,436.20378x + 1.78492$	103.395	0.0741
	long-flame coal	0.96594	$y = -8800.20589x - 2.60558$	73.165	0.0006

Table 4 shows that the inhibitory coal samples of meagre coal, lean coal, gas coal, and long-flame coal had higher activating energy than the respective raw coal samples, with increases of 1.138 KJ·mol<sup>-1</sup>, 23.048 KJ·mol<sup>-1</sup>, 5.23 KJ·mol<sup>-1</sup>, and 5.673 KJ·mol<sup>-1</sup>, respectively. The activating energy of a coal sample is a parameter that measures the spontaneous combustion characteristics, which has an inverse relationship with the tendency of coal to spontaneously combust. Therefore, hydrated phase change materials can reduce the possibility of coal spontaneous combustion. The pre-exponential factor reflects the possibility of collision between activated groups in coal oxidation processes. The bigger the value of the pre-exponential factor, the higher the possibility of collision between activated groups. The pre-exponential factors after inhibition were greater than those before inhibition, as shown in Table 3. However, based on the changes in each coal sample’s activating energy before and after inhibition, it can be inferred that an increase in the pre-exponential factor had less impact on the coal oxidation reaction than an increase in the activating energy.

In summary, hydrated phase change materials had an inhibitory effect on the coal spontaneous combustion effect, which can increase the activating energy of coal and cause delayed oxidation and combustion processes in coal.

## 5. Conclusions

By analyzing the characteristic temperature and weight loss rate, it was found that hydrated phase change materials had effective inhibitory effects on coal samples at different oxidation stages. During the low-temperature stage, a phase change occurred in the material, absorbing heat, isolating the coal from contact with oxygen, reducing the mass loss of inhibited coal samples by 1.6% to 9.3% compared with raw coal, and slowing down the oxidation rate. By analyzing the oxidation characteristic parameters of the raw and inhibited coal samples, it was determined that the addition of hydrated phase change materials can reduce the combustibility indices of meagre coal and lean coal, as well as the comprehensive combustion indices of gas coal and long-flame coal. Furthermore, the activating energy of coal samples was improved after inhibition treatment.

**Author Contributions:** Writing—original draft, F.W.; writing—review and editing, S.S. (Shiliang Shi) and Y.L.; writing—review and editing, S.S. (Shuzhen Shao); validation, supervision, W.G.; investigation, methodology, Y.W. and X.Y. All authors have read and agreed to the published version of this manuscript.

**Funding:** This research was funded by the National Support Plans for the Top of the Notch Youth Talents, grant number 2022QB06801, and the National Natural Science Foundation of China, grant numbers 52174180, 51974119, 52274196, 51974120.

**Institutional Review Board Statement:** Not applicable.

**Informed Consent Statement:** Not applicable.

**Data Availability Statement:** Data will be made available upon request.

**Conflicts of Interest:** The authors declare no conflicts of interest.

## References

1. Ma, Q.; Nie, W.; Yang, S.; Xu, C.; Peng, H.; Liu, Z.; Guo, C.; Cai, X. Effect of spraying on coal dust diffusion in a coal mine based on a numerical simulation. *Environ. Pollut.* **2020**, *264*, 114717. [[CrossRef](#)]
2. Gu, W.; Lu, Y.; Yan, Z.; Wu, F.; Shi, S.; Zhu, S.; Zhang, S.; Guo, X.; Wang, Z.; Wu, X. Spontaneous combustion of coal in regenerated roof and its prevention technology. *Fuel* **2023**, *346*, 128280. [[CrossRef](#)]
3. Chen, J.; Lu, Y.; Tang, G.; Yang, Y.; Shao, S.; Ding, Y. Research and prevention of upper remaining coal spontaneous combustion induced by air leakage in multi-inclination regenerated roof: A case study in the Luwa coal mine, China. *Energy* **2023**, *275*, 127484. [[CrossRef](#)]
4. Dou, G.; Liu, J.; Jiang, Z.; Jian, H.; Zhong, X. Preparation and characterization of a lignin based hydrogel inhibitor on coal spontaneous combustion. *Fuel* **2022**, *308*, 122074. [[CrossRef](#)]
5. Lu, Y.; Shi, S.; Wang, H.; Tian, Z.; Ye, Q.; Niu, H. Thermal characteristics of cement microparticle-stabilized aqueous foam for sealing high-temperature mining fractures. *Int. J. Heat Mass Tran.* **2019**, *131*, 594–603. [[CrossRef](#)]
6. Lu, Y.; Yan, Z.; Shi, S.; Wang, G.; Li, H.; Niu, H.; Guo, Z.; Wang, P. Delineation and prevention of the spontaneous combustion dangerous area of coal in a regenerated roof: A case study in the Zhoujing coal mine, China. *Energy Fuels* **2020**, *34*, 6401–6413. [[CrossRef](#)]
7. Qin, B.; Dou, G.; Wang, Y.; Xin, H.; Ma, L.; Wang, D. A superabsorbent hydrogel–ascorbic acid composite inhibitor for the suppression of coal oxidation. *Fuel* **2017**, *190*, 129–135. [[CrossRef](#)]
8. Pan, D.; Hong, K.; Fu, H.; Zhou, J.; Zhang, N.; Lu, G. Influence characteristics and mechanism of fragmental size of broken coal mass on the injection regularity of silica sol grouting. *Constr. Build. Mater.* **2021**, *269*, 121251. [[CrossRef](#)]
9. Ma, L.; Fan, X.; Wei, G.; Sheng, Y.; Liu, S.; Liu, X. Preparation and characterization of antioxidant gel foam for preventing coal spontaneous combustion. *Fuel* **2023**, *338*, 127270. [[CrossRef](#)]
10. Fang, X.; Wang, H.; Tan, B.; Wang, F.; Shao, Z.Z.; Cheng, G.; Yao, H. Experimental comparison study of CO<sub>2</sub> and N<sub>2</sub> inerted loose coal based on atmospheric pressure gas replacement. *Fuel* **2022**, *328*, 125347. [[CrossRef](#)]
11. Lei, B.; He, B.; Xiao, B.; Du, P.; Wu, B. Comparative study of single inert gas in confined space inhibiting open flame coal combustion. *Fuel* **2020**, *265*, 116976. [[CrossRef](#)]
12. Wu, Z.; Hu, S.; Jiang, S.; He, X.; Shao, H.; Wang, K.; Fan, D.; Li, W. Experimental study on prevention and control of coal spontaneous combustion with heat control inhibitor. *J. Loss Prevent. Proc.* **2018**, *56*, 272–277. [[CrossRef](#)]
13. Xi, Z.; Jin, B.; Jin, L.; Li, M.; Li, S. Characteristic analysis of complex antioxidant enzyme inhibitors to inhibit spontaneous combustion of coal. *Fuel* **2020**, *267*, 117301. [[CrossRef](#)]
14. Zhao, W.; Liu, Y.; Zhao, J.; Cao, H.; Tan, Q.; Zhang, H.; Wang, J. Synthesis of a novel composite component inhibitor and its flame retardant effect on coal. *Case Stud. Therm. Eng.* **2022**, *38*, 102368. [[CrossRef](#)]

15. Huang, Z.; Li, J.; Liu, X.; Gao, Y.; Zhang, Y.; Wang, S.; Li, Z.; Yan, L. Development and Performance Study of a New Physicochemical Composite Inhibitor for Coal Spontaneous Combustion Control. *Combust. Sci. Technol.* **2022**, *194*, 2480–2503. [\[CrossRef\]](#)
16. Huang, Z.; Wang, G.; Ding, H.; Wang, H.; Li, J.; Yu, R.; Gao, Y.; Wang, P. Study on the inhibition performance of double network physicochemical nanocomposite gel inhibitor on coal spontaneous combustion. *Fuel* **2023**, *350*, 128697. [\[CrossRef\]](#)
17. Dong, H.; Hu, X.; Yu, A.; Wang, W.; Zhao, Q.; Wei, H.; Yang, Z.; Wang, X.; Luo, C. Study on the mechanism of an entermorphabased compound inhibitor for inhibiting the spontaneous combustion of coal using in situ infrared spectroscopy and thermal analysis kinetics. *J. Environ. Chem. Eng.* **2023**, *11*, 109577. [\[CrossRef\]](#)
18. Wang, K.; Hu, L.; Deng, J.; Zhang, Y.; Zhang, J. Inhibiting effect and mechanism of polyethylene glycol-Citric acid on coal spontaneous combustion. *Energy* **2023**, *275*, 127522. [\[CrossRef\]](#)
19. Gao, F.; Jia, Z.; Bai, Q.; Dong, J. Characteristics and mechanism of Glutathione in inhibiting coal spontaneous combustion. *Fuel* **2023**, *352*, 129006. [\[CrossRef\]](#)
20. Xue, D.; Hu, X.; Dong, H.; Cheng, W.; Wang, W.; Liang, Y. Examination of characteristics of anti-oxidation compound inhibitor for preventing the spontaneous combustion of coal. *Fuel* **2022**, *310*, 122160. [\[CrossRef\]](#)
21. Pan, R.; Li, X.; Li, H.; Chao, J.; Jia, H.; Ma, Z. Study on the effect of composite hydrogel inhibitors on the heat release characteristics of coal oxidation. *Fuel* **2022**, *309*, 122019. [\[CrossRef\]](#)
22. Gao, A.; Sun, Y.; Hu, X.; Song, S.; Lu, W.; Liang, Y.; He, Z.; Li, J.; Meng, S. Substituent positions and types for the inhibitory effects of phenolic inhibitors in coal spontaneous combustion. *Fuel* **2022**, *309*, 122104. [\[CrossRef\]](#)
23. Tang, Z.; Xu, G.; Yang, S.; Deng, J.; Xu, Q.; Chang, P. Fire-retardant foam designed to control the spontaneous combustion and the fire of coal: Flame retardant and extinguishing properties. *Powder Technol.* **2021**, *384*, 258–266. [\[CrossRef\]](#)
24. Sharma, A.; Tyagi, V.V.; Chen, C.R.; Buddhi, D. Review on thermal energy storage with phase change materials and applications. *Renew. Sustain. Energ. Rev.* **2009**, *13*, 318–345. [\[CrossRef\]](#)
25. Ferrer, G.; Solé, A.; Barreneche, C.; Martorell, I.; Cabeza, L.F. Review on the methodology used in thermal stability characterization of phase change materials. *Renew. Sustain. Energ. Rev.* **2015**, *50*, 665–685. [\[CrossRef\]](#)
26. Da Cunha, J.P.; Eames, P. Thermal energy storage for low and medium temperature applications using phase change materials—A review. *Appl. Energ.* **2016**, *177*, 227–238. [\[CrossRef\]](#)
27. Lu, Y.; Tang, G.; Chen, J.; Shao, S.; Ding, Y.; Li, M.; Wu, F.; Wang, W. Development of composite phase change material for preventing spontaneous combustion of coal and its thermo-physical properties. *Energy Fuels* **2022**, *36*, 3857–3866. [\[CrossRef\]](#)
28. Tang, Y. Experimental investigation of applying MgCl<sub>2</sub> and phosphates to synergistically inhibit the spontaneous combustion of coal. *J. Energy Inst.* **2018**, *91*, 639–645. [\[CrossRef\]](#)
29. Wang, C.; Yuan, J.; Bai, Z.; Hou, Y.; Deng, J.; Xiao, Y. Experimental investigation on using antioxidants to control spontaneous combustion of lignite coal. *Fuel* **2023**, *334 Pt 1*, 126679. [\[CrossRef\]](#)
30. Niu, H.; Yang, Y.; Bu, Y.; Li, S. Study on spontaneous combustion characteristics of coal samples with different pre-oxidized temperatures in secondary oxidation process. *Combust. Sci. Technol.* **2023**, *195*, 1873–1886. [\[CrossRef\]](#)
31. Jia, H.; Yang, Y.; Ren, W.; Kang, Z.; Shi, J. Experimental study on the characteristics of the spontaneous combustion of coal at high ground temperatures. *Combust. Sci. Technol.* **2022**, *194*, 2880–2893. [\[CrossRef\]](#)
32. Di, H.; Wang, Q.; Sun, B.; Sun, M. Reactivity and catalytic effect of coals during combustion: Thermogravimetric analysis. *Energy* **2024**, *291*, 130353. [\[CrossRef\]](#)
33. Si, F.; Zhang, H.; Feng, X.; Dou, J.; Wu, L.; Li, L.; Wang, L.; Zhao, L. Thermal analysis kinetics study of pulverized coal combustion under oxygen-rich atmosphere. *ACS Omega* **2023**, *8*, 33975–33981. [\[CrossRef\]](#) [\[PubMed\]](#)
34. Li, Z.; Wen, H.; Shu, C.-M.; Laiwang, B.; Li, B.; Xiao, Y.; Wei, G. Thermokinetic behavior and microcharacterization of low-rank bitumiteoxidation. *J. Therm. Anal. Calorim.* **2019**, *137*, 1693–1705. [\[CrossRef\]](#)
35. Lin, Y.; Li, Q.; Ji, K.; Li, X.; Yu, Y.; Zhang, H.; Song, Y.; Fu, Y.; Sun, L. Thermogravimetric analysis of pyrolysis kinetics of Shenmu bituminous coal. *React. Kinet. Mech. Cat.* **2014**, *113*, 269–279. [\[CrossRef\]](#)

**Disclaimer/Publisher’s Note:** The statements, opinions and data contained in all publications are solely those of the individual author(s) and contributor(s) and not of MDPI and/or the editor(s). MDPI and/or the editor(s) disclaim responsibility for any injury to people or property resulting from any ideas, methods, instructions or products referred to in the content.